Title: Brain age prediction reveals aberrant brain white matter in schizophrenia and bipolar disorder: A multi-sample diffusion tensor imaging study

Short title: White matter brain age in severe mental illness

Authors: Siren Tønnesen[1*], Tobias Kaufmann[1], Genevieve Richard[1,2,3], Nhat Trung Doan[1], Dag Alnæs[1], Dennis van der Meer[1,4], Jaroslav Rokicki[1,2], Torgeir Moberget[1], Ivan I. Maximov[1,2], Ingrid Agartz[1,5,6], Sofie R. Aminoff[1,7] , Deanna Barch[8,9,10], Justyna Beresniewicz[11,12], Simon Cervenka[6], Alex Craven[11,12], Lena Flyckt[6], Tiril P. Gurholt[1], Unn K. Haukvik[1,13], Kenneth Hugdahl[11,12,14,15], Erik Johnsen[12,16], Erik G. Jönsson[1,6], KaSP[i], Knut K. Kolskår[1,2,3], Kristiina Kompus[11,12], Rune Andreas Kroken[11,12], Trine V. Lagerberg[1], Else-Marie Løberg[12,17,18], Jan Egil Nordvik[19], Anne-Marthe Sanders[1,2,3], Kristine Ulrichsen[1,2,3], Ole A. Andreassen[1], Lars T. Westlye[1,2*]

[1]NORMENT, Institute of Clinical Medicine, University of Oslo, & Division of Mental Health and Addiction, Oslo University Hospital, Oslo, Norway

[2] Department of Psychology, University of Oslo, Norway

[3] Sunnaas Rehabilitation Hospital HF, Nesodden, Norway

[4] School of Mental Health and Neuroscience, Faculty of Health, Medicine and Life Sciences, Maastricht University, The Netherlands

[5] Department of Psychiatry, Diakonhjemmet Hospital, Oslo, Norway

[6] Centre for Psychiatry Research, Department of Clinical Neuroscience , Karolinska Institutet and Stockholm County Council, Stockholm, Sweden

[7] Early Intervention in Psychosis Advisory Unit for South East Norway, Division of Mental Health and Addiction, Oslo University Hospital, Oslo, Norway

[8] Department of Psychological and Brain Sciences, Washington University in St. Louis, St. Louis, USA

[9] Department of Psychiatry, Washington University in St. Louis, St. Louis, USA

[10] Department of Radiology, Washington University in St. Louis, St. Louis, USA

[11] Department of Biological and Medical Psychology, University of Bergen

[12] NORMENT, Haukeland University Hospital, Bergen, Norway

[13]Adult Psychiatry Unit, Department of Mental Health and Addiction, Institute of Clinical Medicine, University of Oslo

[14] Department of Radiology, Haukeland University Hospital, Bergen, Norway

[15] Department of Psychiatry, Haukeland University Hospital, Bergen, Norway

[16] Department of Clinical Medicine (K1), University of Bergen, Norway

[17] Department of Addiction Medicine, Haukeland University Hospital, Bergen, Norway

[18] Department of Clinical Psychology, University of Bergen, Norway

[19] Catosenteret Rehabilitation Center, Son, Norway

* Corresponding authors: Siren Tønnesen (siren.tonnesen@medisin.uio.no) & Lars T. Westlye (l.t.westlye@psykologi.uio.no), postal address: Oslo University Hospital, P.O.Box 4956 Nydalen, 0424 OSLO, Norway, phone: +47 23 02 73 50, Fax: +47 23 02 73 33

Keywords: brain age, DTI, psychosis, schizophrenia, bipolar, machine learning

Word count abstract: 242/250 | Main text: 3907/4000

Number of Figures 2 | Tables: 1 | Supplementary information: 1 document

Abstract (242/250 words)

Background: Schizophrenia (SZ) and bipolar disorders (BD) share substantial neurodevelopmental components affecting brain maturation and architecture. This necessitates a dynamic lifespan perspective in which brain aberrations are inferred from deviations from expected lifespan trajectories. We applied machine learning to diffusion tensor imaging (DTI) indices of white matter structure and organization to estimate and compare brain age between patients with SZ, BD and healthy controls.

Methods: We obtained DTI data from patients with SZ (n=648), BD (n=185) and healthy controls (n=990) across 10 clinical cohorts. We trained six cross-validated models using different combinations of DTI data from 927 controls, and applied the models to estimate individual brain ages in the test sets. We assessed group differences using linear models, accounting for age, sex and scanner.

Results: 10-fold cross-validation revealed high accuracy for all models. Compared to controls, the model including all feature sets significantly over-estimated the age of patients with SZ (d=.29) and BD (d=.15), with similar effects for the other models. Meta-analysis converged on the same findings. Fractional anisotropy (FA) based models were more sensitive than models based on other metrics. Using a reduced set of global features instead of regional features revealed converging results.

Conclusions: Brain age prediction based on DTI provides informative and robust proxies for brain white matter integrity and health. Our results further suggest that white matter aberrations in SZ and BD primarily consist of anatomically distributed deviations from expected lifespan trajectories that generalize across cohorts and scanners.

Introduction

Schizophrenia (SZ) and bipolar (BD) spectrum disorders are severe mental disorders with partly overlapping clinical characteristics and pathophysiology. Both are highly heritable (1) with a substantial neurodevelopmental aetiology (2, 3). Along with evidence of accelerated age-related brain changes in adult patients with SZ (4-6) the neurodevelopmental origin supports a dynamic lifespan perspective in which genetic and biological factors interact with age-related environmental and physiological processes.

Aberrant myelination and brain wiring during adolescence has been included among the neurobiological features of severe mental disorders, and white matter (WM) aberrations have been documented before disease onset (7-11). Brain imaging has shown that normative WM development follows a characteristic non-linear trajectory with peak maturation around the third or fourth decade (12-14). Compared to healthy controls, adult patients with SZ or BD exhibit anatomically distributed group-level differences in various diffusion-based indices of WM structure (15, 16).

Supporting a neurodevelopmental origin, it has been demonstrated that patients with adolescent-onset SZ show WM aberrations (17), and that their developmental trajectory is altered and delayed (18) compared to age-matched normal developing peers. Further, children and adolescents with increased symptom burden, albeit presumably at subclinical levels, were found to exhibit altered diffusion based WM properties compared to peers with low or no symptoms of mental distress (19), highlighting a critical role of WM development in mental health in youths. To which degree group differences observed between adult patients and healthy controls accelerate during the course of the adult lifespan is unclear. The neurodegenerative account of schizophrenia and severe mental illness is debated (20) and lacks unequivocal support from imaging studies (16, 21), but some studies have suggested stronger age-related deterioration of the brain in patients compared to controls (22, 23).

Despite converging evidence of case-control differences both preceding and following disease onset, recent brain imaging studies have documented substantial heterogeneity within patient groups (24, 25). In contrast to conventional group level analyses, brain age prediction using machine learning on imaging features allows for brain-based phenotyping at the individual level, and enables an efficient dimensionality reduction of the neuroimaging data into one or more biologically informative summary measures (26, 27). The discrepancy between an individual's chronological age and predicted brain age, sometimes referred to as the brain age gap (BAG), has been found to be higher in patients with SZ (5, 28, 29) and several other brain disorders (29). However, these previous studies have exclusively used brain grey matter features for brain age prediction. Thus, given the well-documented role of WM aberrations in patients with mental illness (15, 30-32), brain age prediction based on diffusion imaging is clearly warranted.

In order to fill this current gap in the literature, we here compared individual BAGs between patients diagnosed with SZ, BD, and HC using four conventional metrics (fractional anisotropy (FA), mean diffusivity (MD), radial diffusivity (RD) and axial diffusivity (AD)) obtained from diffusion tensor imaging (DTI). We used an independent training set comprising healthy individuals (n=927, aged 18.00-94.96 years) and applied the resulting model in our test sample including patients with SZ (n=648), BD (n=185) and HC (n=990) from 10 independent cohorts. In order to specifically assess the robustness and quantify the heterogeneity of effects across cohorts we adopted a meta-analytic statistical framework.

Since the different DTI-based metrics carry partly independent biological information (33-35), we trained six different models based on various combinations of the DTI metrics, which allowed us to compare prediction accuracy and subsequent group differences between the metrics. Based on converging evidence of widespread WM aberrations in patients with severe mental disorders (15), we hypothesized higher BAG in patients with SZ and BD

compared to HC, with stronger effects in SZ compared to BD. To test the relevance of the varying spatial resolution of the feature sets, which is important to inform the discussion regarding the anatomical specificity of brain WM aberrations, we compared models including various atlas-based tracts of interest (TOIs) with models including only global features. Based on previous studies comparing the prediction accuracy and sensitivity between metrics (16, 27), we hypothesized that FA would enable both high age prediction accuracy and sensitivity to group differences, but remained agnostic concerning the additional value of the remaining features.

Materials and methods

We combined diffusion MRI data from 2750 individuals from 11 sites/studies across 10 different scanners. Figure 1A, Supplementary Figure S1-S2, and Supplementary Table S1-S2 summarise key demographics per cohort. Supplemental Table S3 summarizes the MRI systems and diffusion acquisition protocols.

The dataset was split into a training set and a test set. Supplemental Figure S2 shows the age distribution within each cohort in the training set. Briefly, the training set consisted of 927 HC covering the full adult lifespan (mean age=53.81, s.d.=18.38, range 18.00-94.96 years). The test set comprised 990 HC (mean age=34.70 s.d.=11.24, range=17.52-68.97), 185 patients with BD (mean age=33.12, s.d.=10.53, range=18.40-64.48) and 648 patients with SZ (mean age: 34.49, s.d.=11.40, range=18.00-66.00).

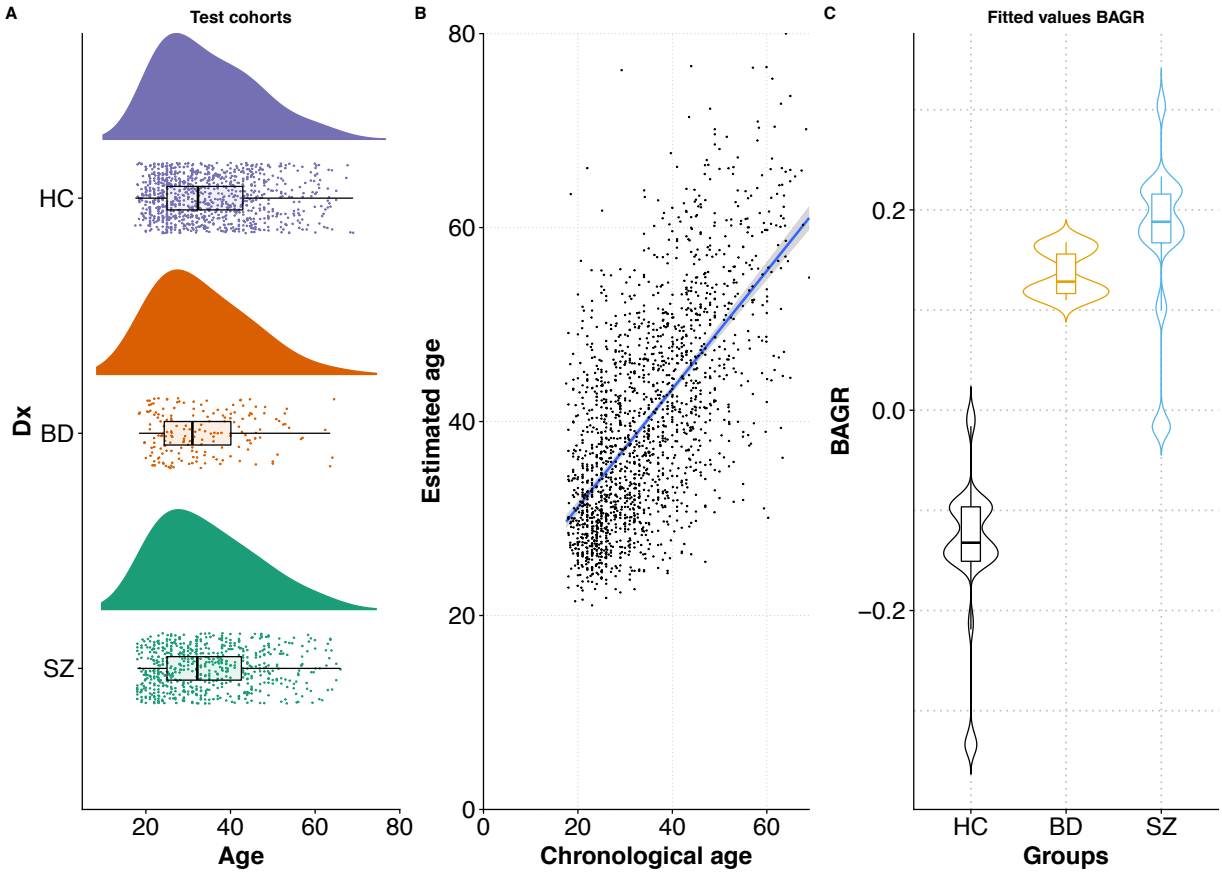

Figure 1. A) Raincloud plot depicting the age distribution for each diagnostic group in the test sets. Density plots are shown on top with data points and boxplot underneath. B) Chronological age plotted as function of estimated brain age using the all features model, the fitted line represents the best linear fit across all subjects using linear regression C) Violin plots showing the distribution of residualized brain age gaps (BAGR) in each group.

MRI acquisition and processing

A summary of MRI acquisition protocol for each cohort is presented in Supplementary Table S3. Imaging analyses were performed using the Oxford Center for Functional Magnetic Resonance Imaging of the Brain (FMRIB) Software Library (FSL) (36-38). To correct for geometrical distortions and eddy currents all cohorts were processed using eddy (http://fsl.fmrib.ox.ac.uk/fsl/fslwiki/eddy) (39, 40). The two cohorts (TOP1 and TOP2) which had collected blip-up/blip-down sequences were additionally processed using topup (http://fsl.fmrib.ox.ac.uk/fsl/fslwiki/topup) (36, 41) prior to eddy. Using an integrated

framework along with correction for susceptibility induced distortions, eddy currents and motion eddy detects and replaces slices affected by signal loss due to bulk motion during diffusion encoding (40).

Fitting of the diffusion tensor was done using dtifit in FSL, yielding conventional DTI metrics, including fractional anisotropy (FA), and mean (MD), radial (RD) and axial (AD) diffusivity. FA, MD, RD and AD maps were further processed using tract-based spatial statistics (TBSS) (42). FA volumes were skull-stripped and aligned to the FMRIB58_FA template supplied by FSL using nonlinear registration (FNIRT) (43). Next, mean FA were derived and thinned to create a mean FA skeleton, representing the center of all tracts common across subjects. We thresholded and binarized the mean FA skeleton at FA>0.2. The procedure was repeated for MD, AD and RD. For each individual, we calculated the mean skeleton FA, MD, AD and RD, as well as mean values within 23 regions of interest (ROIs, Supplemental Table S4) based on two probabilistic white matter atlases provided with FSL, (i.e. the CBM-DTI-81 white-matter labels atlas and the JHU white-matter tractography atlas (44-46)). In total, we derived 96 DTI features per individual including the mean skeleton values.

Quality assessment

Subjects with poor image quality due to subject motion or other visible image artefacts (e.g. due to metal) were removed. Additionally, we employed a multistep quality assessment (QA) procedure (16) that included maximum voxel intensity outlier count (MAXVOX) and tSNR (47) prior to statistical analyses. In short, manual inspection of the flagged datasets after QA suggested adequate quality. Thus, we present results on the full dataset with supplemental results from a stringent QA (see (16) for additional information).

Brain age prediction

We trained six models for age prediction. Our main model included all 96 features across all DTI metrics. To assess metric specificity, we trained four additional models based on all ROIs for each DTI metric (FA, RD, MD or AD). To test the value of including regionally specific information we trained an additional model with only the global mean skeleton feature from all four metrics included.

The following pipeline for brain age prediction was identical for all six models. We used the xgboost framework in R (48) to build the prediction model. The number of rounds (nround), maximum depth (max_depth) and subsample were tuned and optimised using a 5-fold cross validation of the training data, with early stopping if the prediction errors did not improve for 20 rounds. The learning rate (eta) was pre-set to eta=0.01. Besides the default setting, the following parameters were used in the model: nround=1400, max_depth=14.

Prior to implementing the model, we regressed out the main effect of scanner in the entire dataset while accounting for age, age^2, and sex using linear models in R (49). To estimate the reliability of our age prediction model, we used a 10-fold cross-validation procedure within the training sample and repeated the cross-validation step 100 times to provide a robust estimate of model predictive accuracy. Within the same procedure, we tested the performance of our trained model by predicting age in unseen subjects in the test sample. By applying the model to the test sample 100 times we obtain both a mean estimate and an estimate of uncertainty. We then calculated the correlation between the predicted (mean across 100 iterations) and the chronological age as a measure of model performance, in addition to the mean absolute error (MAE, in years) and root mean square error (RSME). For each individual, we calculated the discrepancy between estimated and chronological age, i.e. the BAG. Based on recent recommendation (50) we regressed out the main effect of age on BAG using linear models in R, yielding a residualized BAG (BAGR) used to calculate MAE and RMSE, and for group comparisons across cohorts.

Statistical analyses

Statistical analyses were performed using R (version 3.3.3 (2017-03-06)(49)). We tested for main effects of diagnosis using linear models with BAGR as dependent variable and group, sex and site as independent variables, and performed pairwise group comparisons as appropriate. Using the metafor package (51) in R we adopted a meta-analytic framework in order to assess the heterogeneity and generalizability of the results. A random-effects model was used to weigh the primary studies prior to aggregating the effect size. Effect sizes were aggregated using the estimated marginal means of BAG from each group contrast (HC/SZ, HC/BD and BD/SZ) accounting for age, age^2 and sex. For effect size estimates we used Hedges' *g*. Cochran's heterogeneity statistic *Q* was used to test the homogeneity of effect sizes. A χ^2 test with *k*-1 degrees of freedom was used to examine the significance of Cochran's *Q.* The heterogeneity was quantified using the I^2 statistic, which is sensitive to the degree of inconsistency in results between cohorts.

Results

Brain age predictions

Age prediction in the *training* set using 10-fold cross validation revealed high correlations between chronological and predicted age for the main model including all features (*r*=.855, 95% CI: .845-.865, MAE=7.28, RMSE=9.37).

Figure 1B shows predicted age plotted as a function of chronological age for the test set when using the full feature set, and Table 1 summarizes prediction accuracy for all six models. Age prediction accuracy for the full model was high in HC (r=.593, MAE=7.98, RMSE=10.1), and in patients with BD (r=.576, MAE=8.89, RMSE=11.4), and SZ (r=.553, MAE=9.47, RMSE=12.00). While all models performed relatively well, prediction accuracy

was highest for the full model, and the global mean skeleton model outperformed the ROI based single-metrics models.

Group differences in BAGR

Figure 1C shows the distributions of BAGR within each group, and Table 1 and Supplemental Figure S3 summarize the results from the group comparisons. Briefly, all models revealed significant main effects of group, with higher BAGR in patients with SZ and BD compared to HC. The FA model yielded strongest effect size for the main group effect, although the full and mean skeleton models in addition to FA, MD and RD models revealed similar and converging patterns. All analyses revealed higher BAGR in BD and SZ compared to HC, with effect sizes ranging between d=0.1 and d=0.34. The model based on AD revealed less consistent results, and was the only model not showing significant group differences between SZ and HC.

Table 1
Results from the six brain age models

	Correlation chronological age and predicted age (MAE/RMSE)	BAGR SZ Mean ±sd (95%CI)	BAGR BD Mean ±sd (95%CI)	BAGR HC Mean ±sd (95%CI)	F	*p*	Pairwise comparison	Cohens d HC/SZ, BD/HC, BD/SZ	Cohens d[a] Mean skeleton (HC/SZ, BD/HC, BD/SZ)
All features	.63(8.6/10.9)	-0.73 ±8.79 (-0.05/-1.40)	-1.00±8.37 (0.22/-2.21)	-3.29±7.89 (-2.80-3.78)	21.11	<.001	HC<SZ, HC<BD	-.29/.15/-.04	
Meanskel	.57(9.9/12.8)	-0.48±10.06 (0.30/-1.25)	-1.94±8.86 (-0.66/-3.23)	-3.58±9.41 (-2.99/-4.16)	20.48	<.001	HC<SZ, HC<BD	-.30/.10/-.08	
FA	.52(10.5/13.0)	0.82±9.97 (1.59/0.05)	0.57±9.37 1.93/-0.78)	-2.53±8.65 (-1.99/-3.07)	28.41	<.001	HC<SZ, HC<BD	-.34/.17/-.04	.36/-.17/.18
RD	.44(10.9/13.7)	-0.57±9.84 (0.19/-1.33)	-0.52±8.70 (0.74/-1.78)	-3.37±8.51 (-2.83/-3.90)	21.71	<.001	HC<SZ, HC<BD	-.28/.18/<-.01	-.35/.20/-.14
MD	.50(10.6/13.1)	-1.38±9.46 (-0.65/-2.11)	-0.80±8.46 (0.43/-2.03)	-3.42±8.44 (-2.90/--3.95)	14.48	<.001	HC<SZ, HC<BD	-.22/-.16/.02	-.24/.17/-.06
AD	.56(10.2/12.6)	-2.86±8.54 (-2.20/-3.52)	-2.03±8.39 (-0.81/-3.24)	-3.65±8.33 -3.13/-4.17)	4.60	.010	HC>BD	-.09/-12/.06	<.00/.08/.09

Note. Abbreviations: MAE: Mean estimate error, RMSE: Root mean square error, BAGR: residualised brain age gap, FA: fractional anisotropy, MD: mean diffusivity, RD: radial diffusivity and AD: axial diffusivity.

[a]Cohens d reported for the pairwise group comparisons for mean skeleton

Meta-analysis and heterogeneity in effects between cohorts

Figure 2 shows a forest plot summarizing the results from the meta-analytical approach for the full model. Supplemental Figures S4-S8 show results from the other models. In short, the results revealed significantly higher brain age gap in SZ and BD compared HC with moderate effect sizes. The analysis did not support a group difference in brain age gap between BD and SZ. Whereas the effect sizes varied slightly between cohorts for the full model, the Q and I^2 statistics indicated low and non-significant heterogeneity. Figure S9 shows each cohort's contribution to the heterogeneity and influence on the result from the meta-analysis.

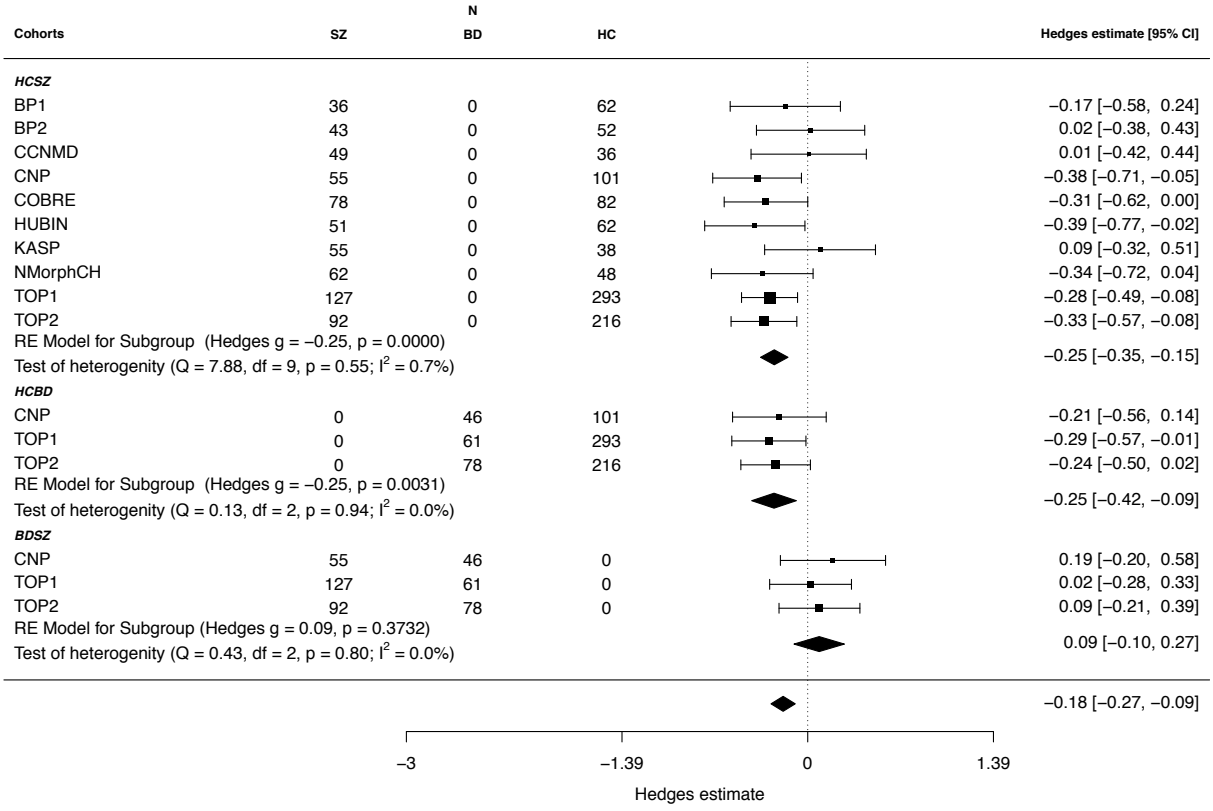

Figure 2. Forest plot summarizing the results from the meta-analytical approach for the all features model. Hedges estimate was used to calculate the effect size.

Quality control

Figure S10 summarises the results from multistep QA. Briefly, higher BAGR was observed in SZ and BD compared to HC across all levels of QA, with highly similar effect sizes.

Discussion

The aetiology of severe mental disorders has a substantial neurodevelopmental component, which is amongst other characteristics reflected in altered brain maturational trajectories during the formative years of childhood and adolescence, and as group-level differences in adult patient populations. Along with evidence of genetic and clinical overlap with several aging-related conditions, including cardiovascular risk factors and increased mortality, the neurodevelopmental account supports the need for a dynamic lifespan perspective in the search for disease mechanisms. Here, in ten different cohorts comprising healthy controls and patients with SZ and BD, we used machine learning to estimate the brain age using DTI based indices of white matter structure and organization. This novel approach yielded five main results. First, in a large independent training set we found high accuracy of brain age prediction across the adult lifespan using DTI features, supporting the feasibility and sensitivity of the approach. Second, applying the model to an independent test set revealed significantly higher brain age gap in patients with SZ and BD compared to HC. Third, follow-up meta-analysis and tests of heterogeneity suggested high consistency across independent cohorts and scanners. Fourth, brain age models based on FA showed higher sensitivity than models based on the other metrics, both alone and combined. Finally, the reduced set of global mean skeleton features compared to a number of regional atlas-based features revealed highly converging results. We next discuss the implications of these findings in more detail.

Brain age prediction provides an informative summary measure that may serve as a proxy for brain integrity and health across normative and clinical populations. Neuroimaging derived white and grey matter phenotypes carry distinct biological information of brain integrity, and tissue-specific brain age models may provide higher sensitivity and specificity to relevant biological processes compared to conventional models based on grey matter features alone (27). DTI has been broadly applied in clinical neuroscience research due to its

proposed sensitivity to microstructural properties of brain tissue. However, whereas previous studies have documented higher brain age in patients with severe mental disorders, these were based on grey matter models only (5, 28, 29). In order to test if previous findings suggesting clinical deviations from normative grey matter trajectories generalize to white matter, we performed brain age prediction using different combinations of DTI based metrics. In line with previous findings (27) we obtained high age prediction accuracy across most models. Supporting previous evidence suggesting that regional DTI based indices of brain aging reflect relatively low-dimensional and global processes (12, 52), we found similar age prediction accuracy for the reduced models comprising global mean skeleton values only compared to the model including the extended set of regional features. Although brain aging shows some regional heterogeneity, these findings demonstrate that the most relevant information required for brain age prediction is captured at the global level. This conjecture is also supported by a recent twin study demonstrating that a large proportion of the estimated heritability of specific tracts is accounted for by a global factor (53).

Likewise, we found that the sensitivity to group differences was not strongly dependent on the inclusion of the full feature set. Indeed, the effect size obtained when comparing patients with SZ and HC were slightly higher for the global mean skeleton model compared to the full model. These findings are in line with recent evidence of anatomically widely distributed group differences between healthy controls and patients with SZ (15). Interestingly, the largest effect when comparing SZ and HC was obtained for the FA only model, supporting the sensitivity of FA to clinical differences in WM properties (15, 16). Higher predicted brain age in the patient groups compared to healthy controls may indicate accelerated brain aging in patients with severe mental disorders. However, our cross-sectional design does not permit us to make any inference about brain aging per se, and previous reports of relatively age-invariant group differences in brain volumetry (21) and DTI indices

(16) suggest that the reported group differences in brain age may in fact reflect differences accumulating already early in life. Unfortunately, due to the current study design with adults only we cannot address the maturational trajectories in the formative years. Although the application of diffusion MRI as the basis for age prediction is novel, higher gray matter brain age has been shown in several brain and mental disorders (29, 54). We extend these previous findings by documenting higher DTI based white matter brain age in both SZ and BD, and, although with moderate effect sizes, we show that the effects are relatively robust across cohorts and scanners, with only minor heterogeneity in effect sizes between cohorts.

We found no significant difference in BAGR between BD and SZ, supporting previous evidence of partly overlapping clinical and biological characteristics between these two diagnostic categories (16, 55, 56). While the current results support the existence of a common set of mechanisms across disorders, future studies utilizing a broader range of imaging modalities in combination with specific genetic, clinical (symptoms, cognitive function etc) and biological phenotypes may allow for the identification of specific diagnostic signatures and sub-groups. However, inherent limitations associated with the classical case-control design in mental health research have recently been emphasized using neuroimaging data (24, 25). In particular, the current lack of biologically informed diagnostic criteria should motivate future studies to consider alternative approaches to promote a novel clinical nosology based both on symptomatology and data-driven clustering (57) as well as brain-based and biological phenotypes cutting across diagnostic boundaries.

Our results document robust group level deviances in white matter structure manifesting as older-appearing brains in patients with severe mental disorders compared to their healthy peers. Whereas DTI based markers are sensitive to a range of different biological and anatomical characteristics, the current specificity does not allow for inference on the distinct neurobiological mechanisms involved. Myelin integrity and myelin packing density

are among the proposed candidate mechanisms for observed changes in DTI metrics (34, 58, 59), but the specificity is low, and the current results probably reflect a combination of different neurobiological processes and macroanatomical differences. Previous evidence has implicated myelin-related abnormalities and neuroinflammation both in the pathophysiology of severe mental disorders and in brain aging (60-63). Future studies may benefit from the inclusion of advanced diffusion based models based on multi-shell diffusion MRI allowing for stronger inference on the microstructural milieu of the brain tissue, including microstructural indices based on different diffusion scalar metrics (e.g., Neurite Orientation Dispersion and Density Imaging (NODDI) (64, 65), diffusion kurtosis imaging (DKI) (66), white matter tract integrity (WMTI) (67) and restriction spectrum imaging (RSI) (68)).

In line with previous findings of widely distributed effects in well-powered studies of brain aging (12) and schizophrenia (15), we found similar age prediction accuracy and subsequent group differences in brain age for the model including only global mean skeleton values and the model including a range of regional informative values extracted from various atlas-based tracts and regions of interest. Although specific symptoms and clinical traits may map preferentially onto specific neuroanatomical subsystems (see e.g. (19)), these novel results suggest that a large proportion of the relevant variance associated with age and corresponding deviations in the patients groups are captured by primarily global brain processes, with relevance for our understanding of the anatomical heterogeneity and dimensionality of brain aging and severe mental illness.

In addition to the anatomical distribution of effects, the spatiotemporal dynamics of brain development and aging and their deviations in patients with mental disorders remain unclear. The individual level onset and rate of the group-level deviations from the normative white matter trajectory is unknown and can only be inferred using longitudinal designs covering sensitive periods of neurodevelopment. Previous studies have shown both delayed

neurodevelopment during adolescence (18) and accelerated aging in adulthood (5) in patients with severe mental disorders. Whereas these observations are not mutually exclusive, future studies should aim at disentangling the lifespan dynamics, e.g. by including individuals with a wider age-range and pursuing longitudinal designs in individuals across a wide range of functional levels and risk. The latter may be particularly pertinent to disentangle primary disease-related mechanisms and secondary factors related to the disease, including medication and life-style factors such as nutrition, physical activity, education etc. Unfortunately, although possible effects of psychotropic drugs on the brain is a topic of great interest and importance (69-71), in common with other studies employing a cross-sectional and non-randomised design the current design does not allow us to make inference about the effects of medication and other clinical and lifestyle factors on brain age, which should be investigated by future and properly designed studies. Meanwhile, previous studies reporting associations with medication status in smaller samples need to be interpreted in light of the recent lack of significant associations in the largest DTI study to date (15).

In conclusion, in this multi-sample study including patients from 10 different cohorts we report higher brain age in patients with SZ and BD compared to HC using various DTI-based indices of white matter structure and organization. Although the effect sizes were modest, our unique design allowed us to specifically quantify the heterogeneity and robustness of effects across cohorts and scanners, supporting that brain age prediction using diffusion MRI is a sensitive marker in the clinical neurosciences.

Acknowledgements

This work was funded by the South-Eastern Norway Regional Health Authority (2014097, 2015073, 2016083, 2016044), the Western Norway Regional Health Authority (911820, 911679),the Research Council of Norway (213700, 204966, 249795, 223273, 213727), KG

Jebsen Stiftelsen and the European Commission's 7th Framework Programme (#602450, IMAGEMEND). KaSP was supported by grants from the Swedish Medical Research Council (SE: 2009-7053; 2013-2838; SC: 523-2014-3467), the Swedish Brain Foundation, Åhlén-siftelsen, Svenska Läkaresällskapet, Petrus och Augusta Hedlunds Stiftelse, Torsten Söderbergs Stiftelse, the AstraZeneca-Karolinska Institutet Joint Research Program in Translational Science, Söderbergs Königska Stiftelse, Professor Bror Gadelius Minne, Knut och Alice Wallenbergs stiftelse, Stockholm County Council (ALF and PPG), Centre for Psychiatry Research, KID-funding from the Karolinska Institutet. Data collection and sharing for this project was provided by the Cambridge Centre for Ageing and Neuroscience (CamCAN). CamCAN funding was provided by the UK Biotechnology and Biological Sciences Research Council (grant number BB/H008217/1), together with support from the UK Medical Research Council and University of Cambridge, UK. CCNMD was supported through NIH Grants P50 MH071616 and R01 MH56584. CNP was supported by the Consortium for Neuropsychiatric Phenomics (NIH Roadmap for Medical Research grants UL1-DE019580, RL1MH083268, RL1MH083269, RL1DA024853, RL1MH083270, RL1LM009833, PL1MH083271, and PL1NS062410). The HUBIN project was supported by the Swedish Research Council (2006- 2992, 2006-986, K2007-62X-15077-04-1, 2008-2167, K2008-62P- 20597-01-3. K2010-62X-15078-07-2, K2012-61X-15078-09-3, 2017-00949, K2015-62X-15077-12-3), the regional agreement on medical training and clinical research between Stockholm County Council and the Karolinska Institutet, the Knut and Alice Wallenberg Foundation. StrokeMRI was supported by the Research Council of Norway (249795, 248238), the South-Eastern Norway Regional Health Authority (2014097, 2015044, 2015073, 2016083), and the Norwegian ExtraFoundation for Health and Rehabilitation (2015/FO5146). Data collection and sharing for the NMorphCH project was funded by NIMH

grant A R01 MH056584. The BergenPsykose project was supported by the European Research Council (ERC AdG) (693124), and Western Norway Health-Authorities (912045).

[i] Members of the Karolinska Schizophrenia Project (KaSP): Farde L[1], Flyckt L[1], Engberg G[2], Erhardt S[2], Fatouros-Bergman H[1], Cervenka S[1], Schwieler L[2], Piehl F[3], Agartz I[1,4,5], Collste K[1], Victorsson P[1], Malmqvist A[2], Hedberg M[2], Orhan F[2], Sellgren C[2]

[1]Centre for Psychiatry Research, Department of Clinical Neuroscience, Karolinska Institutet, & Stockholm County Council, Stockholm, Sweden; [2]Department of Physiology and Pharmacology, Karolinska Institutet, Stockholm, Sweden; [3]Neuroimmunology Unit, Department of Clinical Neuroscience, Karolinska Institutet, Stockholm, Sweden; [4]NORMENT, Division of Mental Health and Addiction, University of Oslo, Oslo, Norway; [5]Department of Psychiatry Research, Diakonhjemmet Hospital, Oslo, Norway

References

1. Pettersson E, Lichtenstein P, Larsson H, Song J, Agrawal A, Borglum AD, et al. (2018): Genetic influences on eight psychiatric disorders based on family data of 4 408 646 full and half-siblings, and genetic data of 333 748 cases and controls. *Psychological medicine*.1-8.
2. O'Shea KS, McInnis MG (2016): Neurodevelopmental origins of bipolar disorder: iPSC models. *Molecular and cellular neurosciences*. 73:63-83.
3. Bora E, Ozerdem A (2017): Meta-analysis of longitudinal studies of cognition in bipolar disorder: comparison with healthy controls and schizophrenia. *Psychological medicine*. 47:2753-2766.
4. Kochunov P, Ganjgahi H, Winkler A, Kelly S, Shukla DK, Du X, et al. (2016): Heterochronicity of white matter development and aging explains regional patient control differences in schizophrenia. *Human brain mapping*.
5. Schnack HG, van Haren NE, Nieuwenhuis M, Hulshoff Pol HE, Cahn W, Kahn RS (2016): Accelerated Brain Aging in Schizophrenia: A Longitudinal Pattern Recognition Study. *The American journal of psychiatry*. 173:607-616.
6. Kochunov P, Hong LE (2014): Neurodevelopmental and neurodegenerative models of schizophrenia: white matter at the center stage. *Schizophrenia bulletin*. 40:721-728.
7. Paus T, Keshavan M, Giedd JN (2008): Why do many psychiatric disorders emerge during adolescence? *Nature reviews Neuroscience*. 9:947-957.
8. Carletti F, Woolley JB, Bhattacharyya S, Perez-Iglesias R, Fusar Poli P, Valmaggia L, et al. (2012): Alterations in white matter evident before the onset of psychosis. *Schizophrenia bulletin*. 38:1170-1179.
9. Paillère Martinot ML, Lemaitre H, Artiges E, Miranda R, Goodman R, Penttilä J, et al. (2013): White-matter microstructure and gray-matter volumes in adolescents with subthreshold bipolar symptoms. *Molecular psychiatry*. 19:462.
10. Barnea-Goraly N, Chang KD, Karchemskiy A, Howe ME, Reiss AL (2009): Limbic and corpus callosum aberrations in adolescents with bipolar disorder: a tract-based spatial statistics analysis. *Biological psychiatry*. 66:238-244.

11. Insel TR (2010): Rethinking schizophrenia. *Nature*. 468:187-193.
12. Westlye LT, Walhovd KB, Dale AM, Bjornerud A, Due-Tonnessen P, Engvig A, et al. (2010): Life-span changes of the human brain white matter: diffusion tensor imaging (DTI) and volumetry. *Cerebral cortex*. 20:2055-2068.
13. Rathee R, Rallabandi VP, Roy PK (2016): Age-Related Differences in White Matter Integrity in Healthy Human Brain: Evidence from Structural MRI and Diffusion Tensor Imaging. *Magnetic resonance insights*. 9:9-20.
14. Kochunov P, Williamson DE, Lancaster J, Fox P, Cornell J, Blangero J, et al. (2012): Fractional anisotropy of water diffusion in cerebral white matter across the lifespan. *Neurobiology of aging*. 33:9-20.
15. Kelly S, Jahanshad N, Zalesky A, Kochunov P, Agartz I, Alloza C, et al. (2017): Widespread white matter microstructural differences in schizophrenia across 4322 individuals: results from the ENIGMA Schizophrenia DTI Working Group. *Molecular psychiatry*.
16. Tonnesen S, Kaufmann T, Doan NT, Alnaes D, Cordova-Palomera A, Meer DV, et al. (2018): White matter aberrations and age-related trajectories in patients with schizophrenia and bipolar disorder revealed by diffusion tensor imaging. *Scientific reports*. 8:14129.
17. Douaud G, Smith S, Jenkinson M, Behrens T, Johansen-Berg H, Vickers J, et al. (2007): Anatomically related grey and white matter abnormalities in adolescent-onset schizophrenia. *Brain*. 130:2375-2386.
18. Douaud G, Mackay C, Andersson J, James S, Quested D, Ray MK, et al. (2009): Schizophrenia delays and alters maturation of the brain in adolescence. *Brain*. 132:2437-2448.
19. Alnaes D, Kaufmann T, Doan NT, Cordova-Palomera A, Wang Y, Bettella F, et al. (2018): Association of Heritable Cognitive Ability and Psychopathology With White Matter Properties in Children and Adolescents. *JAMA psychiatry*. 75:287-295.
20. Rund BR (2009): Is schizophrenia a neurodegenerative disorder? *Nordic journal of psychiatry*. 63:196-201.
21. Moberget T, Doan NT, Alnaes D, Kaufmann T, Cordova-Palomera A, Lagerberg TV, et al. (2018): Cerebellar volume and cerebellocerebral structural covariance in schizophrenia: a multisite mega-analysis of 983 patients and 1349 healthy controls. *Molecular psychiatry*. 23:1512-1520.
22. Cropley VL, Klauser P, Lenroot RK, Bruggemann J, Sundram S, Bousman C, et al. (2017): Accelerated Gray and White Matter Deterioration With Age in Schizophrenia. *The American journal of psychiatry*. 174:286-295.
23. Kochunov P, Glahn DC, Rowland LM, Olvera RL, Winkler A, Yang YH, et al. (2012): Testing the Hypothesis of Accelerated Cerebral White Matter Aging in Schizophrenia and Major Depression. *Biological psychiatry*.
24. Wolfers T, Doan NT, Kaufmann T, Alnaes D, Moberget T, Agartz I, et al. (2018): Mapping the Heterogeneous Phenotype of Schizophrenia and Bipolar Disorder Using Normative Models. *JAMA psychiatry*. 75:1146-1155.
25. Alnaes D, Kaufmann T, van der Meer D, Cordova-Palomera A, Rokicki J, Moberget T, et al. (2019): Brain Heterogeneity in Schizophrenia and Its Association With Polygenic Risk. *JAMA psychiatry*.
26. Cole JH, Marioni RE, Harris SE, Deary IJ (2018): Brain age and other bodily 'ages': implications for neuropsychiatry. *Molecular psychiatry*.
27. Richard G, Kolskaar K, Sanders A-M, Kaufmann T, Petersen A, Doan NT, et al. (2018): Assessing distinct patterns of cognitive aging using tissue-specific brain age prediction based on diffusion tensor imaging and brain morphometry. *bioRxiv*.

28. Koutsouleris N, Davatzikos C, Borgwardt S, Gaser C, Bottlender R, Frodl T, et al. (2014): Accelerated brain aging in schizophrenia and beyond: a neuroanatomical marker of psychiatric disorders. *Schizophrenia bulletin*. 40:1140-1153.
29. Kaufmann T, van der Meer D, Doan NT, Schwarz E, Lund MJ, Agartz I, et al. (2018): Genetics of brain age suggest an overlap with common brain disorders. *bioRxiv*.
30. Klauser P, Baker ST, Cropley VL, Bousman C, Fornito A, Cocchi L, et al. (2016): White Matter Disruptions in Schizophrenia Are Spatially Widespread and Topologically Converge on Brain Network Hubs. *Schizophrenia bulletin*.
31. Ellison-Wright I, Bullmore E (2009): Meta-analysis of diffusion tensor imaging studies in schizophrenia. *Schizophrenia research*. 108:3-10.
32. Patel S, Mahon K, Wellington R, Zhang J, Chaplin W, Szeszko PR (2011): A meta-analysis of diffusion tensor imaging studies of the corpus callosum in schizophrenia. *Schizophrenia research*. 129:149-155.
33. Assaf Y, Pasternak O (2008): Diffusion tensor imaging (DTI)-based white matter mapping in brain research: a review. *Journal of molecular neuroscience : MN*. 34:51-61.
34. Song SK, Sun SW, Ju WK, Lin SJ, Cross AH, Neufeld AH (2003): Diffusion tensor imaging detects and differentiates axon and myelin degeneration in mouse optic nerve after retinal ischemia. *NeuroImage*. 20:1714-1722.
35. Alba-Ferrara LM, de Erausquin GA (2013): What does anisotropy measure? Insights from increased and decreased anisotropy in selective fiber tracts in schizophrenia. *Frontiers in integrative neuroscience*. 7:9.
36. Smith SM, Jenkinson M, Woolrich MW, Beckmann CF, Behrens TE, Johansen-Berg H, et al. (2004): Advances in functional and structural MR image analysis and implementation as FSL. *NeuroImage*. 23 Suppl 1:S208-219.
37. Woolrich MW, Jbabdi S, Patenaude B, Chappell M, Makni S, Behrens T, et al. (2009): Bayesian analysis of neuroimaging data in FSL. *NeuroImage*. 45:S173-186.
38. Jenkinson M, Beckmann CF, Behrens TE, Woolrich MW, Smith SM (2012): Fsl. *NeuroImage*. 62:782-790.
39. Andersson JL, Sotiropoulos SN (2016): An integrated approach to correction for off-resonance effects and subject movement in diffusion MR imaging. *NeuroImage*. 125:1063-1078.
40. Andersson JL, Graham MS, Zsoldos E, Sotiropoulos SN (2016): Incorporating outlier detection and replacement into a non-parametric framework for movement and distortion correction of diffusion MR images. *NeuroImage*. 141:556-572.
41. Andersson JL, Skare S, Ashburner J (2003): How to correct susceptibility distortions in spin-echo echo-planar images: application to diffusion tensor imaging. *NeuroImage*. 20:870-888.
42. Smith SM, Jenkinson M, Johansen-Berg H, Rueckert D, Nichols TE, Mackay CE, et al. (2006): Tract-based spatial statistics: voxelwise analysis of multi-subject diffusion data. *NeuroImage*. 31:1487-1505.
43. Jenkinson M, Bannister P, Brady M, Smith S (2002): Improved optimization for the robust and accurate linear registration and motion correction of brain images. *NeuroImage*. 17:825-841.
44. Hua K, Zhang J, Wakana S, Jiang H, Li X, Reich DS, et al. (2008): Tract probability maps in stereotaxic spaces: analyses of white matter anatomy and tract-specific quantification. *NeuroImage*. 39:336-347.
45. Mori S, Wakana S, Nagae-Poetscher L, van Zijl P (2005): *MRI atlas of human white matter*. Amsterdam (The Netherlands: Elsevier.

46. Wakana S, Caprihan A, Panzenboeck MM, Fallon JH, Perry M, Gollub RL, et al. (2007): Reproducibility of quantitative tractography methods applied to cerebral white matter. *NeuroImage*. 36:630-644.
47. Roalf DR, Quarmley M, Elliott MA, Satterthwaite TD, Vandekar SN, Ruparel K, et al. (2016): The impact of quality assurance assessment on diffusion tensor imaging outcomes in a large-scale population-based cohort. *NeuroImage*. 125:903-919.
48. Chen T, He T, Benesty M, Khotilovich V, Tang Y (2015): Xgboost: extreme gradient boosting. *R package version 04-2*.1-4.
49. R Development Core Team (2014): R: A language and environment for statistical computing. Vienna, Austria: R Foundation for Statistical Computing.
50. Le TT, Kuplicki RT, McKinney BA, Yeh H-W, Thompson WK, Paulus MP, et al. (2018): A Nonlinear Simulation Framework Supports Adjusting for Age When Analyzing BrainAGE. *Frontiers in Aging Neuroscience*. 10:317.
51. Viechtbauer W (2010): Conducting meta-analyses in R with the metafor package. *Journal of statistical software*. 36.
52. Penke L, Maniega SM, Murray C, Gow AJ, Valdés Hernández MC, Clayden JD, et al. (2010): A General Factor of Brain White Matter Integrity Predicts Information Processing Speed in Healthy Older People. *The Journal of Neuroscience*. 30:7569.
53. Gustavson DE, Hatton SN, Elman JA, Panizzon MS, Franz CE, Hagler DJ, Jr., et al. (2019): Predominantly global genetic influences on individual white matter tract microstructure. *NeuroImage*. 184:871-880.
54. Kuhn T, Kaufmann T, Doan NT, Westlye LT, Jones J, Nunez RA, et al. (2018): An augmented aging process in brain white matter in HIV. *Human brain mapping*. 39:2532-2540.
55. Owen MJ, Craddock N, Jablensky A (2007): The genetic deconstruction of psychosis. *Schizophrenia bulletin*. 33:905-911.
56. Hill SK, Reilly JL, Harris MS, Rosen C, Marvin RW, Deleon O, et al. (2009): A comparison of neuropsychological dysfunction in first-episode psychosis patients with unipolar depression, bipolar disorder, and schizophrenia. *Schizophrenia research*. 113:167-175.
57. Maglanoc LA, Landrø NI, Jonassen R, Kaufmann T, Córdova-Palomera A, Hilland E, et al. (2019): Data-Driven Clustering Reveals a Link Between Symptoms and Functional Brain Connectivity in Depression. *Biological Psychiatry: Cognitive Neuroscience and Neuroimaging*. 4:16-26.
58. Song SK, Yoshino J, Le TQ, Lin SJ, Sun SW, Cross AH, et al. (2005): Demyelination increases radial diffusivity in corpus callosum of mouse brain. *NeuroImage*. 26:132-140.
59. Checa A, Malmqvist A, Flyckt L, Schwieler L, Samuelsson M, Skogh E, et al. (2018): Cerebrospinal fluid levels of sphingolipids associate with disease severity in first episode psychosis patients. *Schizophrenia research*. 199:438-441.
60. Hakak Y, Walker JR, Li C, Wong WH, Davis KL, Buxbaum JD, et al. (2001): Genome-wide expression analysis reveals dysregulation of myelination-related genes in chronic schizophrenia. *Proceedings of the National Academy of Sciences of the United States of America*. 98:4746-4751.
61. Stedehouder J, Kushner SA (2016): Myelination of parvalbumin interneurons: a parsimonious locus of pathophysiological convergence in schizophrenia. *Molecular psychiatry*.
62. van Kesteren CF, Gremmels H, de Witte LD, Hol EM, Van Gool AR, Falkai PG, et al. (2017): Immune involvement in the pathogenesis of schizophrenia: a meta-analysis on postmortem brain studies. *Translational psychiatry*. 7:e1075.

63. van den Ameele S, Fuchs D, Coppens V, de Boer P, Timmers M, Sabbe B, et al. (2018): Markers of Inflammation and Monoamine Metabolism Indicate Accelerated Aging in Bipolar Disorder. *Frontiers in psychiatry*. 9:250.
64. Nazeri A, Mulsant BH, Rajji TK, Levesque ML, Pipitone J, Stefanik L, et al. (2016): Gray Matter Neuritic Microstructure Deficits in Schizophrenia and Bipolar Disorder. *Biological psychiatry*.
65. Rae CL, Davies G, Garfinkel SN, Gabel MC, Dowell NG, Cercignani M, et al. Deficits in neurite density underlie white matter structure abnormalities in first-episode psychosis. *Biological psychiatry*.
66. Jensen JH, Helpern JA, Ramani A, Lu H, Kaczynski K (2005): Diffusional kurtosis imaging: the quantification of non-gaussian water diffusion by means of magnetic resonance imaging. *Magn Reson Med*. 53:1432-1440.
67. Fieremans E, Jensen JH, Helpern JA (2011): White matter characterization with diffusional kurtosis imaging. *NeuroImage*. 58:177-188.
68. White NS, Leergaard TB, D'Arceuil H, Bjaalie JG, Dale AM (2013): Probing tissue microstructure with restriction spectrum imaging: Histological and theoretical validation. *Human brain mapping*. 34:327-346.
69. Kuroki N, Kubicki M, Nestor PG, Salisbury DF, Park HJ, Levitt JJ, et al. (2006): Fornix integrity and hippocampal volume in male schizophrenic patients. *Biological psychiatry*. 60:22-31.
70. Cheung V, Cheung C, McAlonan GM, Deng Y, Wong JG, Yip L, et al. (2008): A diffusion tensor imaging study of structural dysconnectivity in never-medicated, first-episode schizophrenia. *Psychological medicine*. 38:877-885.
71. Bollettini I, Barberi I, Poletti S, Radaelli D, Pirovano A, Lorenzi C, et al. (2015): Sterol Regulatory Element Binding Transcription Factor-1 Gene Variation and Medication Load Influence White Matter Structure in Schizophrenia. *Neuropsychobiology*. 71:112-119.